Pacific Northwest
NATIONAL LABORATORY

PNNL-35985

Surface Modification of Alloys for Low-cost Corrosion Protection in Marine Environment

Interim Project Report of Marine Energy Sapling Project

April 2024

Sridhar Niverty (sridhar.niverty@pnnl.gov)
George Bonheyo (george.bonheyo@pnnl.gov)
Aashish Rohatgi (aashish.rohatgi@pnnl.gov)

U.S. DEPARTMENT OF ENERGY

Prepared for the U.S. Department of Energy
under Contract DE-AC05-76RL01830

DISCLAIMER

PACIFIC NORTHWEST NATIONAL LABORATORY
operated by
BATTELLE
for the
UNITED STATES DEPARTMENT OF ENERGY
under Contract DE-AC05-76RL01830

Printed in the United States of America

Available to DOE and DOE contractors from the
Office of Scientific and Technical Information,
P.O. Box 62, Oak Ridge, TN 37831-0062;
ph: (865) 576-8401
fax: (865) 576-5728
email: reports@adonis.osti.gov

Available to the public from the National Technical Information Service
5301 Shawnee Rd., Alexandria, VA 22312
ph: (800) 553-NTIS (6847)
email: orders@ntis.gov <https://www.ntis.gov/about>
Online ordering: http://www.ntis.gov

PNNL-35985

Surface Modification of Alloys for Low-cost Corrosion Protection in Marine Environment

Interim Project Report of Marine Energy Sapling Project

April 2024

Sridhar Niverty (sridhar.niverty@pnnl.gov)
George Bonheyo (george.bonheyo@pnnl.gov)
Aashish Rohatgi (aashish.rohatgi@pnnl.gov)

Prepared for
the U.S. Department of Energy
under Contract DE-AC05-76RL01830

Pacific Northwest National Laboratory
Richland, Washington 99354

Executive Summary

This work was undertaken as part of a Sapling project funded by the Marine Energy Program within the DOE's Water Power Technologies Office. The goal of this work was to explore the role of laser surface processing (LSP) for improving the corrosion and more importantly, the biofouling resistance of Al alloy surfaces. Existing antifouling approaches such as painting/coatings, or using corrosion resistant materials, suffer from durability issues, are expensive, and potentially contain environmentally toxic constituents. LSP offers a swift and effective alternative to protect the material by locally modifying the surface of the material. The efficacy and performance of LSP'd surfaces depends on the alloy system and laser process parameters. The challenge lies in optimizing the laser process parameters to best protect the surfaces of interest from corrosion and biofouling.

In this study, LSP was performed using three different laser powers (1.28W, 2.34W, 3.12W) on AA6061 aluminum. Corrosion experiments were performed on the non-LSP and LSP samples by exposing them to natural seawater (in Sequim, WA) and in 3.5 wt.% NaCl solution (in Richland, WA) for durations of 3 and 6 months. Gravimetry, optical and electron microscopy were employed to quantify the changes occurring to the surface and sub-surface regions of the material. Based on these tests, key observations are:

- LSP AA6061 in seawater showed a complete absence of sub-surface intergranular corrosion. On the other hand, non-LSP AA6061 showed ample evidence of sub-surface intergranular corrosion and corrosion induced grain dissolution.

- LSP AA6061 (3.12W) tested for 6 months in seawater showed ~40% lower % weight change per unit area due to biofouling, as compared to non-LSP AA6061.

These results show that LSP can help reduce susceptibility of Al alloys to biofouling and corrosion in seawater. LSP is also not harmful to local marine life and non-chemical in nature. Further analysis is required to understand the microstructural mechanisms that lead to these improved surface behaviors. As LSP can be applied locally, and in a desired location without affecting the remainder of the material, its applicability at joints and welds of components and structures in marine energy applications should be explored.

Acknowledgments

We would like to acknowledge Prof. Hongtao Ding and his team at the University of Iowa for their help in fabricating laser processed samples. We would also like to acknowledge the following PNNL staff for their help in executing this project: Robert Seffens (corrosion testing, sample handling and data analysis), Loreen Lamoureux (corrosion testing, sample handling and data analysis), Noelani Boise (corrosion testing and sample handling), and Tanvi A Ajantiwalay (SEM Analysis). PNNL is a multiprogram national laboratory operated by Battelle for the DOE under Contract DEAC05-76RL01830.

Acronyms and Abbreviations

ASM	American Society for Metals
ASTM	American Society for Testing and Materials
BSE-SEM	Backscattered electron – scanning electron microscopy
DOD	Department of Defense
DOE	Department of Energy
EDS	Energy dispersive spectroscopy
IGC	Intergranular corrosion
LSP	Laser surface processing
Mg	Magnesium
NaCl	Sodium chloride
Nd:YAG	Neodymium-doped yttrium aluminum garnet
Ni	Nickel
ONR	Office of Naval Research
PI	Principal investigator
PNNL	Pacific Northwest National Laboratory
SE	Secondary electron imaging
SEM	Scanning electron microscopy

Contents

Figures

1.0 Background

This work was undertaken as part of a Sapling project funded by the Marine Energy Program within the DOE's Water Power Technology Office. The goal of this work was to explore the role of laser assisted surface modifications to enhance the corrosion resistance of existing commercial Al alloys exposed to marine environments and investigate its benefits in mitigating biofouling. Traditional corrosion protection strategies utilize polymer based coatings that unfortunately exhibit durability issues and need to be reapplied periodically, incurring significant operational and maintenance costs. Additionally, coatings can also contain organic biocides, metallic biocides (e.g., Cu), and other chemicals to prevent biofouling that can be potentially harmful to other marine life in general. The use of polymer based coatings also releases plastics into the ocean water, further contributing to the issue of microplastics proliferation. In a recent work published by project PI Aashish Rohatgi, LSP was shown to significantly enhance the corrosion resistance of a magnesium (Mg) AZ31B alloy in salt water [Jana et al., 2021]. This encouraging result with Mg raised an interesting possibility if similar corrosion protection could also be achieved with aluminum (Al) alloys, specifically those that are used in marine environments. Thus, this Sapling project was proposed with the goal of exploring laser surface processing (LSP) as a novel, corrosion protection technique with the secondary goal of exploring if LSP also affects the propensity for biofouling. This work is a follow-up to a seedling project wherein laser surface processing was employed on AA6061, mild steel, and stainless steel and showed promising improvements to corrosion resistance. Laser surface processing locally modifies materials surfaces without having a direct impact on their bulk properties. LSP is non-chemical, i.e., it does not involve paints/coatings and through its effect on materials' surface chemistry and microstructure, has the potential as an alternative corrosion protection technique that can alleviate some of the durability and cost challenges of existing corrosion protection approaches. Additionally, it is benign to marine life around it. Therefore, this Sapling was undertaken to explore the corrosion behavior of laser surface processed 6061 Al alloy.

2.0 Literature Review

2.1 Corrosion and Biofouling Challenges

Corrosion is a major challenge to marine energy structures. Structures such as offshore wind farms, ship hulls, ship superstructures, helicopters, and jets are susceptible to corrosion attack due to either immersion within seawater, exposure to salt sprays, erosion corrosion at the water line or exposure to dry-wet cycling. The presence of dissimilar material combinations (e.g., dissimilar fastener-plate material configurations) can lead to preferential corrosion attack near the faying surface / interface. Among Al alloys, 6XXX and 5XXX alloys are usually used in seawater applications. AA6061 (Al-Mg-Si rich) is a widely used Al alloy that is used in the T6 temper. T6 temper refers to a specific heat treatment cycle (solution treatment → quenching → peak aging) that maximizes its strength and hardness. Mechanistically, AA6061-T6 undergoes intergranular corrosion due to the presence of a network of Mg_2Si precipitates at the grain boundaries. Also, the Al-Fe-Si intermetallic particles in the alloy's matrix are known to behave cathodically relative to the matrix in a neutral or acidic saltwater environment. This indicates that the Al matrix will preferentially dissolve around the Al-Fe-Si particles.

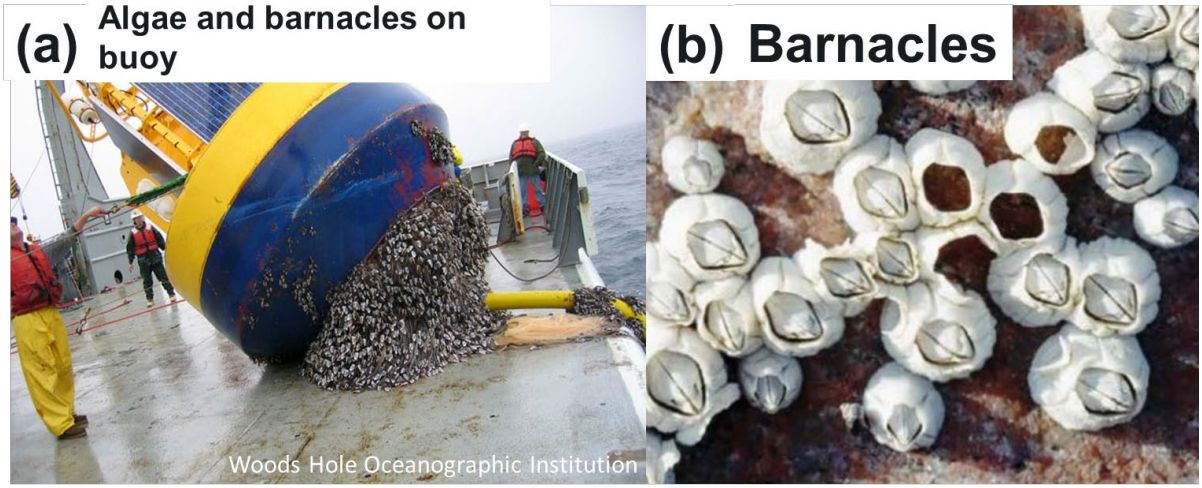

Figure 1: Examples of biofouling on marine structures, (a) Algae and barnacles at the bottom of a research buoy. SOURCE: Woods Hole Oceanographic Institution [2], (b) Closeup image of barnacles on a ship hull [3].

In addition to corrosion, biofouling caused by marine life in seawater also contributes to the degradation of marine structures and deterioration of performance. Specifically, biofouling is caused by the growth of marine organisms such as algae, barnacles, and diatoms on the surface of structures when exposed to marine environments. Figure 1 (a) and (b) show examples of growth of organisms (algae and barnacles on a buoy in figure 1(a) and barnacles on a ship hull in figure 1(b)) on marine structures. The combination of biofouling and corrosion has been observed in several marine energy devices such as wind turbines (floating/planted to sea floor) [4], wave energy convertors [5], marine heat exchangers [6], and foundation structures for marine energy devices [7]. The population of microbial organisms contributing to biofouling depends on geographic location, water temperatures, depth of sampling, salinity, wave current velocity, nutrient availability, etc., and whether the structure is static or moving and floating or fixed. Marine energy structures are usually made of steels due to their strength and weight that can be

advantageous in fixed and static marine energy structures. However, steels are susceptible to crevice corrosion, can rapidly corrode if the sacrificial anode is depleted and can undergo biofouling on their surface [5,8]. This leads to increased weight of the structure, increased operation and maintenance (O&M) costs, and increased drag on the boats/ships that leads to greater energy consumption. In parts such as ship propellers, biofouling via barnacle formation on the surface leads to significant reductions in efficiency. A study by the coast guard office of operational and environments in 2010 estimated the total cost associated with biofouling to be $120 B per year.

To combat biofouling, coatings containing organotin biocides were developed for marine applications. Organotin biocides are compounds of Tin containing organic groups that are attached to the tin as a C-Sn bond. They are very effective at protecting structures from biofouling and exhibit a predictable performance and degradation/leach rate. However, they are highly toxic to marine life and lead to negative health effects on multiple organs in marine organisms [9,10]. In response to this concern, copper (Cu)-rich coatings have been used since the 1980s as Cu has a natural anti-fouling property. These coatings contain 40-60 wt.% of Cu (thus adding significant weight to the coating) and have a service life ranging from a few months up to 5 years [11]. While Cu-rich coatings are relatively less harmful compared to organo-tin biocides, they can still negatively affect local marine life in harbors by sloughing causing high quantities of Cu to be released into the water over time [12]. In response, local and regional standards are being developed with the aim of controlling Cu leaching rate from marine paints into the environment. An example of this is the California leaching rate standard set at 9.5 $\mu g/cm^2$/day, which was enacted by the California Department of Pesticide Regulation in 2018 [13,14]. These factors make the overall use of Cu-rich coatings expensive, heavy, and harmful to the marine life near docks [11].

In the light of the above mentioned corrosion and biofouling challenges, this report investigates the viability of laser surface processing as a technique to improve the corrosion and biofouling resistance of AA6061 aluminum alloy.

2.2 Commercial Laser Systems

To date, PNNL's work on the use of LSP for surface protection has been done using a Nd:YAG laser system in a collaborator's research lab and it is not known a priori if other types of lasers would be equally effective for surface protection. At the lower end of energy (10's W to 100 W), laser systems (e.g., those sold by www.Laserstar.net) for surface marking can cost between $30K-$100K. At the higher energy end, for example, PNNL recently purchased a laser system with a 2 kW Ytterbium fiber laser with ~ 2 ft. x ~1 ft. x ~1 ft. x-y-z travel and maximum velocity (x-y) of 5 m/s.

3.0 Experimental Procedure

3.1 Test Materials and Coupons

Plates of commercially available 6061 Al (T6 temper) (~1.58 mm thick) were procured as test materials representative of those used in the marine energy industry. They were cut into ~1.25” x 1.25” sized coupons and provided to our collaborator (University of Iowa) for LSP. Non-LSP samples served as the baseline to compare against the LSP samples.

3.2 Laser Surface Processing (LSP)

LSP was performed using a Q-Switched Nd:YAG nanosecond laser (Spectra-Physics Quanta-Ray Lab-150, wavelength 1064 nm) with an energy per pulse on the order of several hundreds of mJ/pulse. The laser repetition rate was 10 pulses per second with a pulse duration of 6~8 ns. The samples were immersed in water during LSP and the laser scan head was rastered on the top surface of the sample to create a ~1” x 1” laser processed area. The samples were processed at laser powers of 1.28 W, 2.34 W and 3.12 W and shipped back to PNNL for corrosion testing. The laser parameters were selected based on results from the prior seedling. Examples of samples without and with laser surface processing can be seen in figures 2 (a) and (b).

3.3 Corrosion Testing

3.3.1 General sample preparation

The sample preparation procedure is broken into 6 steps as follows:

- **Cut:** The specimens were marked and cut from the sheet into ~1.25” x ~1.25” sized coupon samples. A hole was drilled into the samples in the top left corner. Figure 2(c) shows a schematic of the sample after a hole is drilled.

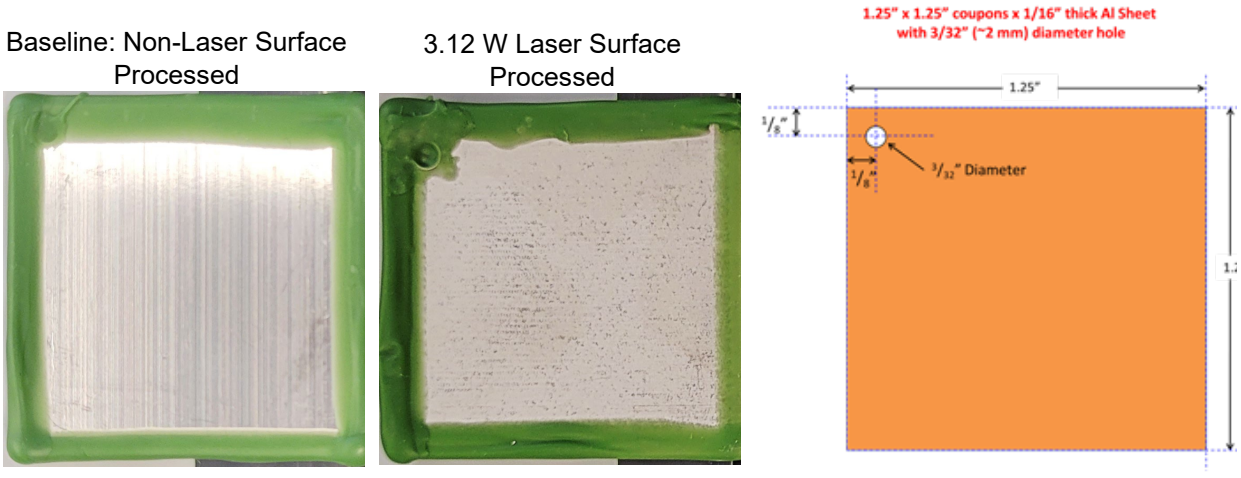

Figure 2: (a) and (b) show a comparison of the surfaces of AA6061 coupons without and with laser surface processing. (c) Schematic showing dimensions of the sample and the hole (diameter- 3/32”) drilled.

- **Clean:** The samples were placed in a beaker and filled with acetone.
  1) The beaker was placed into an ultrasonic bath and cleaned for at least 20 minutes. The samples were then placed onto a dry clean cloth and blow dried.
  2) The samples were transferred to a new clean cloth and rinsed with ethanol and air dried. Blow drying was used as necessary.
  3) The samples were placed into labeled bags and transferred to the weighing station.

- **Uncoated Weight:** Weights of the samples were recorded with a resolution of +/-1 mg.

- **Coat:** Prior to corrosion exposure, the sample edges and non-LSP areas were masked using a PeelSeal Green maskant. It is a high viscosity liquid coating that dries in air and acts as a barrier coating, thereby allowing us to expose a pre-determined area to the environment. This ensured that only the designated areas were exposed to the corrosive environment. The desired area for performing corrosion on the sample is 1”x1”. Thus, the sample was coated with the maskant at a distance of 0.125” from each edge. The samples were cured at room temperature for a duration of 8 hours.

- **Coated Weight:** Weights of the samples were recorded once again with a resolution of +/-1 mg.

- **Preparation for Testing:** The samples were suspended in solution using a fishing line attached to the sample. The fishing line was tied into a loop long enough to suspend each sample in either the 3.5 wt.% NaCl solution (Richland) or in the seawater (Sequim). Coupons were imaged after wrapping with PeelSeal Green by placing on a Kaiser RS 2 XA imaging platform equipped with dual RB 5020 DS LED lamps (Figure 3A), and a Nikon D5300 equipped with a 105 mm AF-S Micro Nikkor lens. Coupons were placed on the platform with a ruler in the image frame to establish scale (Figure 3B), and then an image of both sides of the coupon was recorded. The images were used to measure the metal area exposed to the corrosion medium. Following this step, the coupons were immersed in the corrosive environment (seawater or 3.5% NaCl solution).

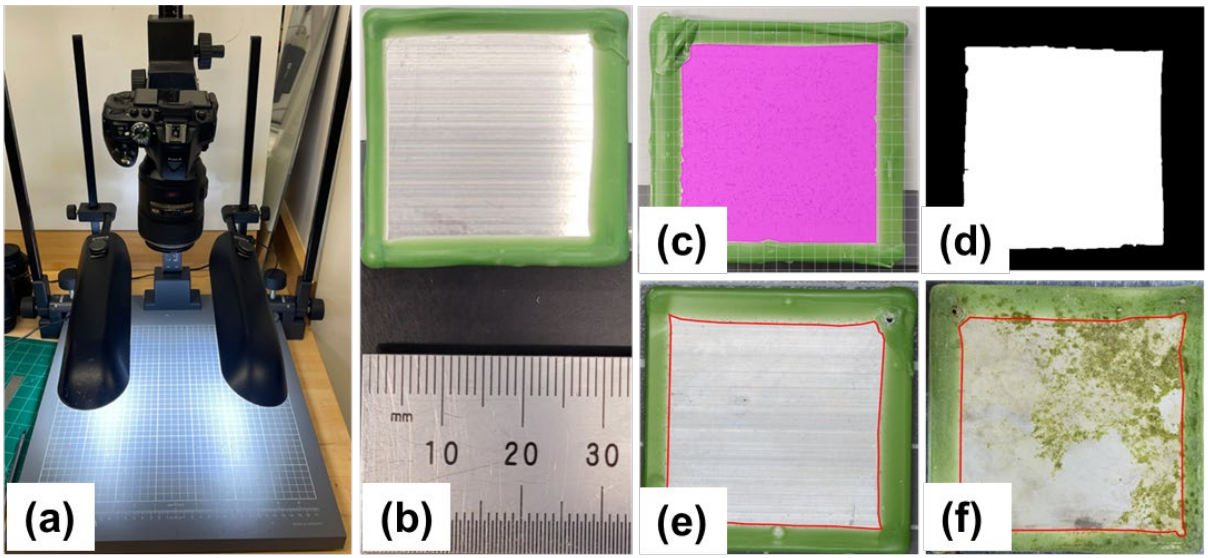

Figure 3: Determination of area exposed to saline or seawater. (a) Nikon D5300 camera and dual LED Kaiser lighting platform, (b) Coupons were placed on lighting platform with a ruler to establish scale for every photo, (c) Area determination using an online application (SketchandCalc [1]) for irregular area determination. Highlighted pink area is the region of interest for which the area is calculated, (d). Determining area with Adobe Photoshop using contrast and thresholding and scale setting. (e) Determination of area using Fiji (Image J) by outlining the region of interest and setting a scale. (f) Image of a biofouled coupon from seawater tank and determination of area using ImageJ.

3.3.2 Lab Salt water (3.5 wt.% NaCl solution) testing

Baseline Al Test Setup

A fishing line string was attached through the pre-drilled hole and tied off so the specimen could be suspended in the solution (Figure 4(a)). 3.5 wt. % NaCl solution was prepared by dissolving 35.24 g of granular NaCl in 1000 mL of deionized (DI) water. The specimens were fully submerged and suspended via a plastic stirring rod. The beaker was then covered in parafilm to minimize evaporation and maintain the original salt concentration. DI water was added periodically to maintain the total volume and NaCl concentration of the solution (Figure 4(b)). The specimens were immersed for a duration of 3 months and 6 months.

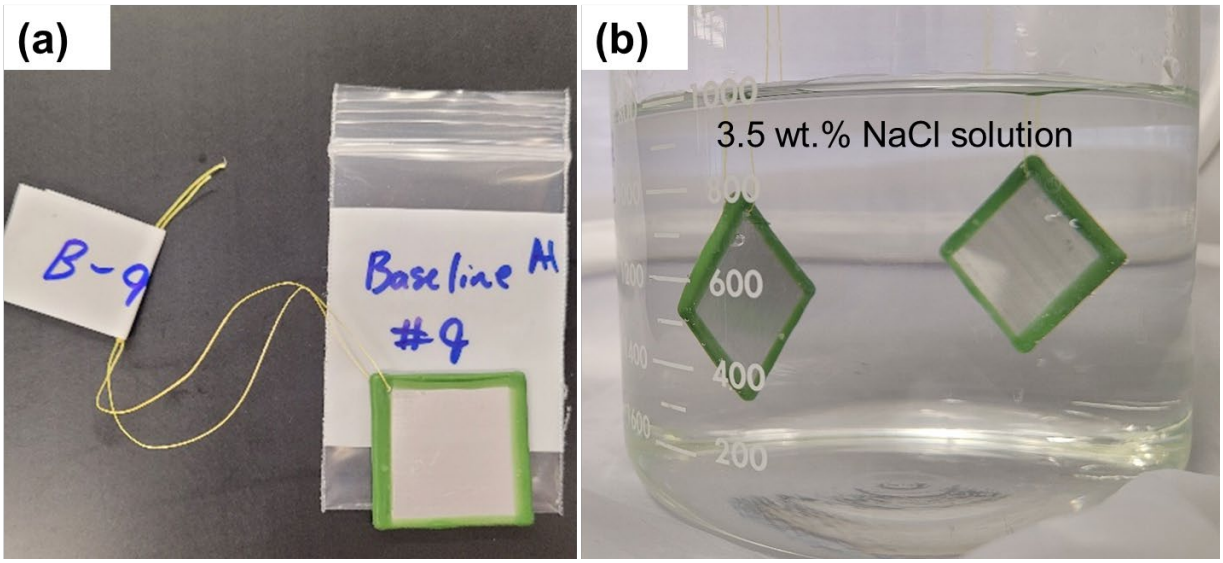

Figure 4: (a) Sample with the peel seal green coating covering its edges and string passing through the corner hole of the sample, (b) Samples immersed in lab 3.5 wt.% NaCl solution. SOURCE: PNNL

3.3.3 Natural Seawater exposure testing

Exposure to seawater and determination of biofouling was conducted by hanging coupons in outdoor marine tanks at the PNNL Marine and Coastal Research Laboratory in Sequim, Washington. Coupons were strung with braided fishing line and hung from PVC struts in an outdoor tank with full exposure to sunlight and constant flow of natural seawater drawn from Sequim Bay. To assess biofouling, triplicate coupons were pulled out at a period of 3 and 6 months. To determine the coupon weight after a given test duration, the coupons were removed from the tank and passed three times through a Dyson hand dryer to remove loose water. The wet weight of the coupon was then recorded in a pre-weighed aluminum sample holder. After recording the wet weight, coupons were placed in individual pre-weighed aluminum sample holders and then dried in a 50 °C oven for 24 hours. The dry weight of coupons was then recorded, and coupons weight boats were packaged in individual containers and then shipped back to PNNL Richland campus for further characterization.

Gravimetric analysis was performed to compare the samples exposed to lab 3.5 wt.% NaCl solution and natural seawater. Specific samples were also imaged using a Keyence VR6000 optical profilometer and using Scanning Electron Microscopy (SEM). Secondary Electron Imaging (SE), Backscatter Electron Imaging (BSE) and Energy Dispersive Spectroscopy (EDS) were performed on the samples to study the extent of corrosion and biofouling presence and to estimate elemental distribution of corrosion features of interest. The surface of the samples was studied to investigate the biofouling remnant on the surface. The cross-sections of the samples were also mounted, polished, and imaged in SEM to study sub-surface corrosion.

3.4 Microscopy:

Scanning Electron Microscopy was employed to visualize the surface and sub-surface corrosion. Additionally, it was used to examine biofouling on the surface of the natural seawater exposed

samples. To visualize the corrosion attack on the surface of the exposed samples, the samples were imaged as-exposed and cleaned without any destructive surface preparation such as polishing. To investigate and compare sub-surface corrosion progress in the non-LSP and 3.12 W LSP conditions, the samples were cross-sectioned, mounted in epoxy, polished to a 1µm diamond finish and imaged. Large area montages of the sample were acquired, and several high resolution images and corresponding EDS maps were acquired at features of significance to corrosion.

4.0 Results

The samples exposed to 3.5 wt.% NaCl solution in the lab at Richland showed signs of corrosion on the surface. On the other hand, the samples exposed to the seawater environment showed signs of both corrosion and biofouling. Decoupling the role of corrosion and biofouling on the weight change of the samples is a challenge as the precise mechanism by which biofouling supports or inhibits corrosion in AA6061 is unknown. Therefore, as a first assumption, we estimated the contribution of biofouling to weight change by subtracting the weight change only due to corrosion (obtained from lab tests at PNNL) from the weight change seen in seawater exposed samples.

Gravimetric Analysis: Biofouling behavior of laser surface processed (LSP) Al coupons and non-laser surface processed (non-LSP) coupons was compared. Figure 5 (a) compares the surfaces of the baseline non-LSP, and LSP coupons after 6 months of seawater testing. The green colored features on the surface of the samples indicate the presence and growth of green algae due to biofouling. Initial observations clearly show lower coverage of green algae on the LSP samples' surface indicating lower biofouling compared to the non-LSP samples.

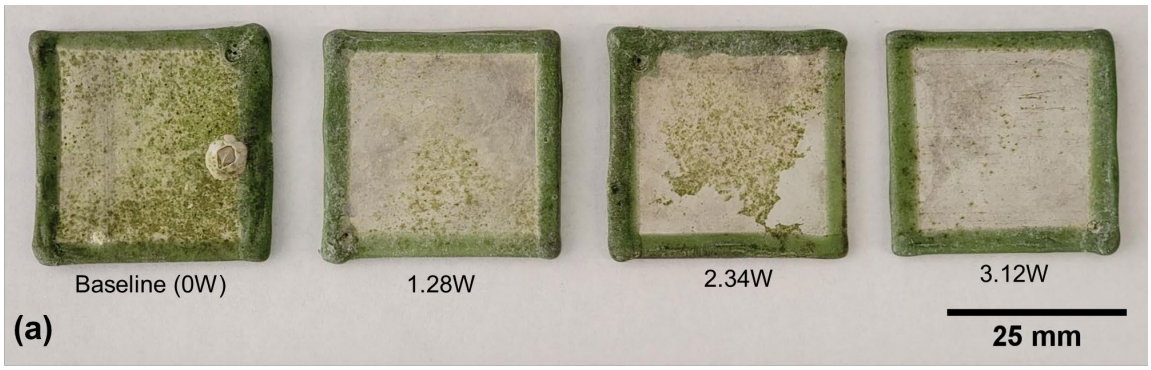

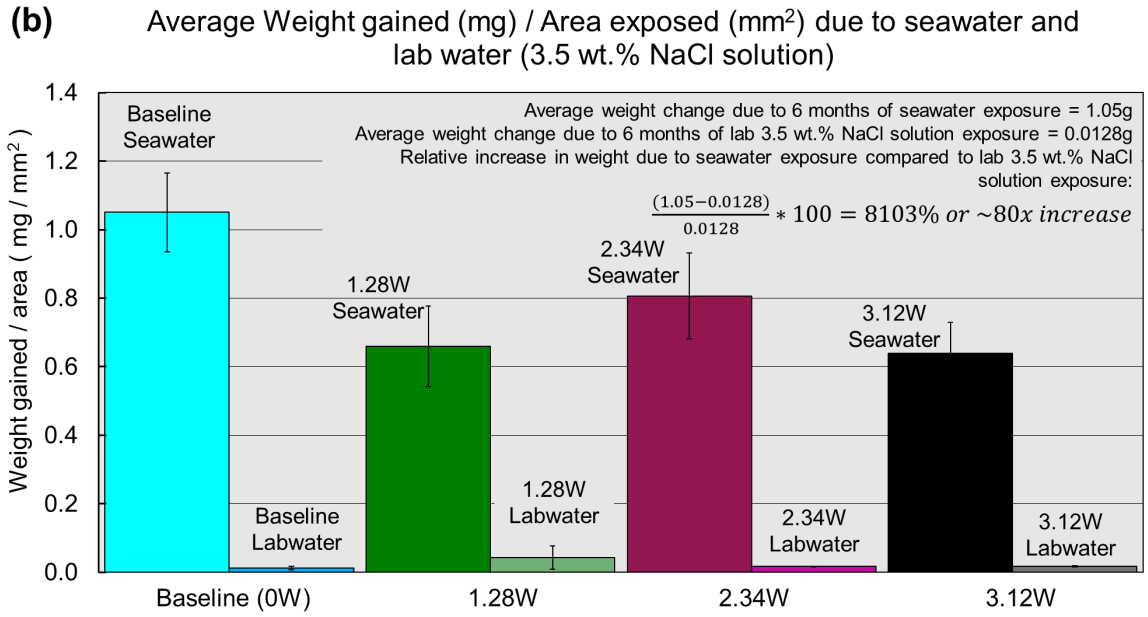

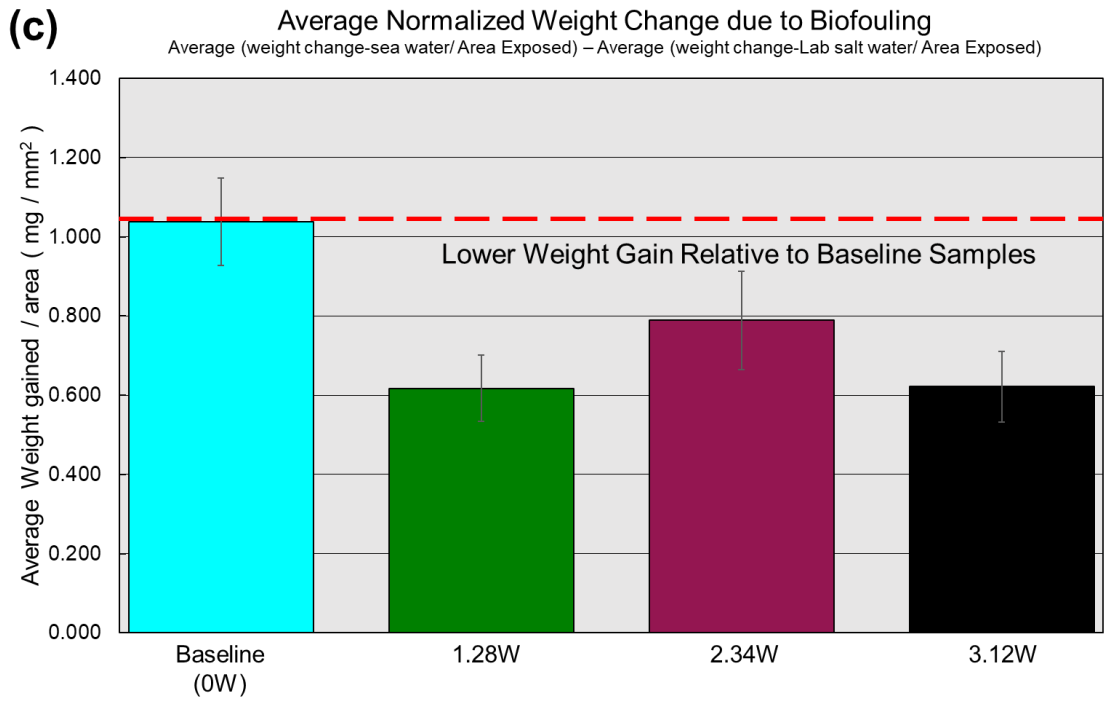

Figure 5: Comparison of weight changes in non-LSP baseline, LSP 1.28 W, LSP 2.34 W and LSP 3.12 W corroded samples (a) Low magnification photographs of the samples after 6 months of seawater exposure, (b) Normalized mass gained in both, lab 3.5 wt.% NaCl solution (corrosion only) and seawater (corrosion and biofouling), in each sample type, (c) Weight change only due to biofouling obtained by subtracting the weight change due to lab 3.5 wt.% NaCl solution from the weight change due to seawater exposure. Dashed red line shows the avg weight gained in the baseline sample. The laser treated samples show lower weight gain relative to baseline samples.

Additionally, Figure 5(b) shows the weight gain due to seawater exposure (corrosion and biofouling) and lab 3.5 wt.% NaCl solution, respectively. In the baseline non-LSP samples, the weight changes due to seawater exposure testing (corrosion + biofouling) are ~80x greater than the weight changes measured due to exposure to lab 3.5 wt.% NaCl solution (corrosion only) over 6 months of corrosion. The LSP samples also show a lower weight change compared to non-LSP baseline samples. Specifically, the 3.12W LSP sample showed the lowest weight change under both lab water and seawater exposure conditions. The weight change measurements combined with the images of the samples indicate that LSP samples show lower biofouling than non-LSP baseline samples.

To demonstrate the effect of biofouling on sample weight, figure 5(c) shows a bar chart comparing the normalized (by area of exposure in each sample) percent weight gain purely due to biofouling measured in the LSP and non-LSP samples. The chart indicates that under the current test conditions, the LSP samples show up to ~40% lower weight gain (i.e., lower biofouling) than the baseline non-LSP samples. This suggests the efficacy of LSP in mitigating biofouling in Al in marine environments.

Optical and Electron Microscopy:

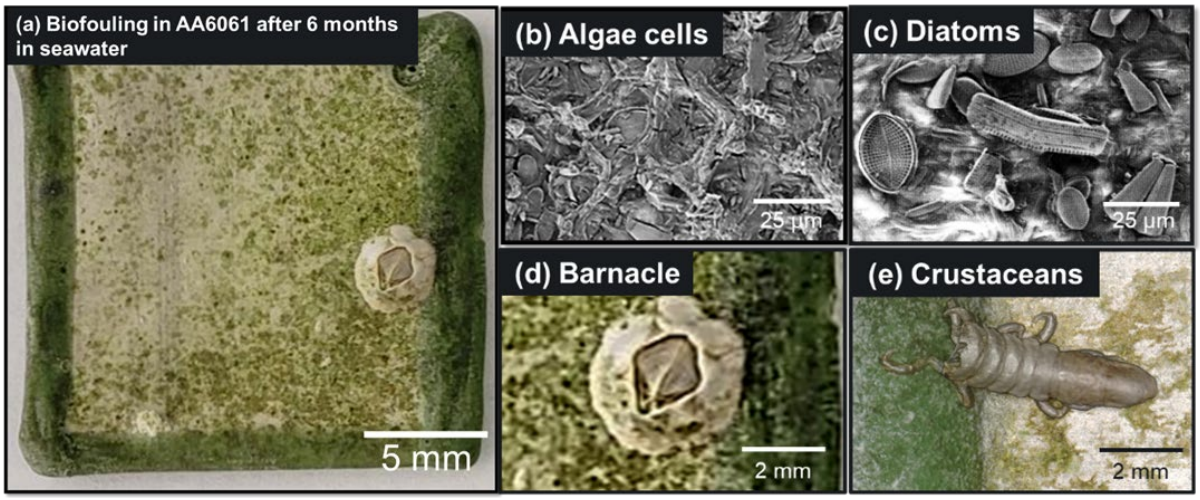

Figure 6: Biofouling in baseline aluminum (Al) alloy AA6061 in seawater for 6 months and the variety of biofouling observed on the surface, (a) AA6061 coupon showing biofouling on the surface, (b) Green algae cells, (c) Diatoms, (d) Barnacles, (e) Crustaceans. (b) and (c) are SEM images. Source: PNNL

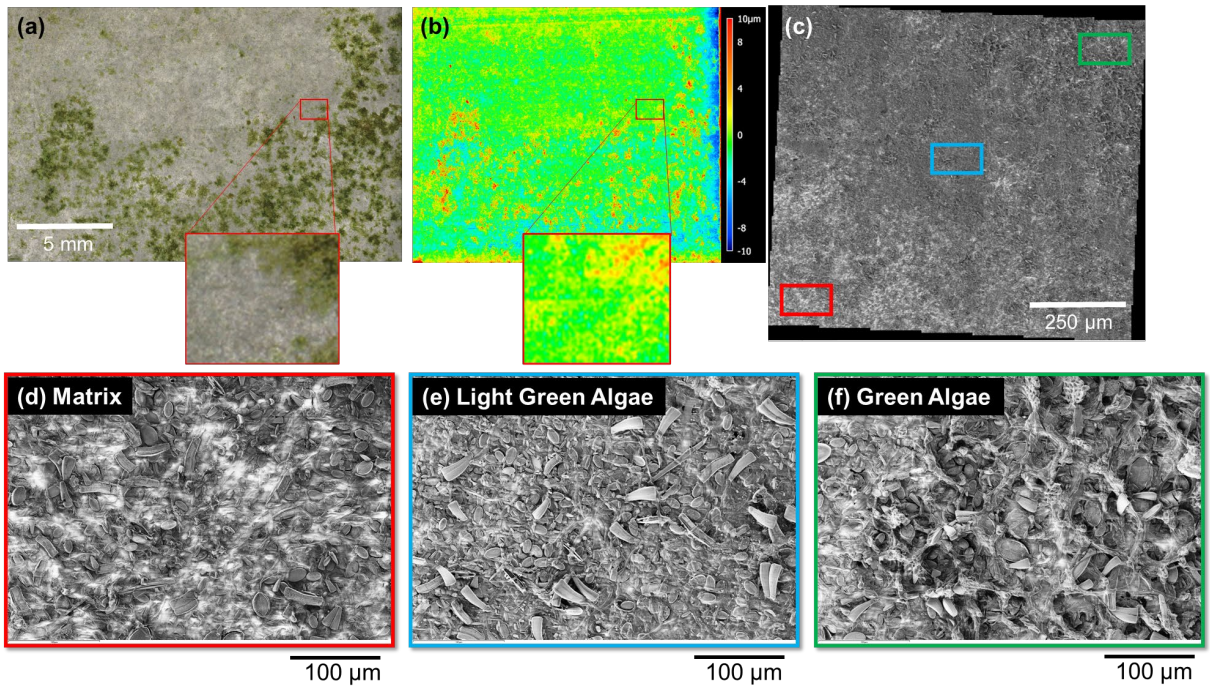

Figure 7: (a) Optical micrograph of a baseline sample corroded in seawater for 6 months, (b) Topography map of the sample and region shown in (a). Both (a) and (b) show an inset image each where SEM analysis was performed, (c) Low resolution BSE-SEM image showing an area containing the algae and the matrix, (d) Inset red box from (c) showing the matrix of the sample containing the presence of diatoms and a biofilm covering the surface, (e) Inset blue box showing the presence of diatoms and petal like algae structures, (f) Inset green box showing the presence of green algae cells and diatom.

Figure 6 (a) shows an example of a baseline non-LSP sample that was exposed to 6 months in seawater. Figures 6 (b)-(e) show examples of organisms that were observed on the surface. From largest to smallest, we observed the presence of barnacles, crustaceans, cell-like structures of green algae and diatoms. Additionally, the surface of the Al is not visible as it is covered with a thin layer of biofilm. This highlights the complexity involved in analyzing and deconvoluting their role on surface corrosion as a whole and individually and is beyond the scope of current work.

Scanning Electron Microscopy (SEM) was performed on seawater exposed coupons from the baseline non-LSP and 3.12 W LSP conditions. Specifically, coupons exposed for a duration of 6 months in seawater were compared. Figure 7 shows the surface of a baseline non-LSP sample exposed to seawater for 6 months. Highlighted in Figure 7 (a) and (b) are the optical micrograph and topography map of an exposed surface. The surface exhibits discoloration with light grey and dark grey patches which could be indicative of the biofilm that forms on the surface almost immediately upon immersion in seawater. They are also accompanied by the presence of green algae on the surface. The green algae are measured to have a maximum height of ~10 μm from the surface. Figure 7(c) shows a low resolution BSE-SEM image from the inset region from (a) and (b). This region is characterized by the presence of green algae on the top right edge of the sample and transitions into the matrix at the bottom left of the image. Higher resolution figures (d), (e) and (f) show the biofilm covered matrix, light green algae that lies in between the biofilm covered matrix and the green algae, and green algae, respectively. Each region is characterized by the presence of diatoms. The light green algae region also contains petal-like algae structures, and the green algae contains cell-like structures that distinguish it from the other regions. Due to the coverage of the biofilm on the entire sample's surface and the presence of dense algae and diatom rich regions, it is not possible to make conclusions about the nature and extent of Al corrosion taking place in the material by looking at the top view of the surface.

To investigate the extent of corrosion taking place, the cross sections of the baseline sample and the 3.12 W LSP sample exposed to 6 months of seawater environments were investigated. Figure 8(a) shows a representative backscattered electron image of the cross section of a baseline non-LSP coupon and its corresponding EDS map. The images show sub-surface intergranular corrosion (IGC) present in the alloy. The images show one of several examples of such IGC observed in the microstructure. The IGC is characterized by the presence of a sub-surface network of corrosion following the grain boundaries in the aluminum alloy matrix. Additionally, some of the grains have also undergone corrosion/dissolution leaving behind corrosion product. The corrosion product is composed of Al and O as shown in the EDS maps. Figure 8(b) shows the sub-surface corrosion behavior of the 3.12 W LSP sample. No sub-surface corrosion and specifically, no intergranular corrosion was observed in samples subjected to this laser condition even after 6 months of corrosion. The observed absence of sub-surface corrosion in the form of intergranular corrosion could indicate that the LSP is effective at modifying the surface chemistry and the sub-surface microstructure so as to develop a resistance to sub-surface corrosion. However, further testing and characterization is required to clarify the mechanism(s) behind the improvement in corrosion resistance.

This observation of the absence of sub-surface corrosion combined with the overall ~40% lower corrosion and biofouling induced weight change is encouraging evidence that LSP can enhance the resistance of 6061 Al to both, biofouling, and corrosion attack.

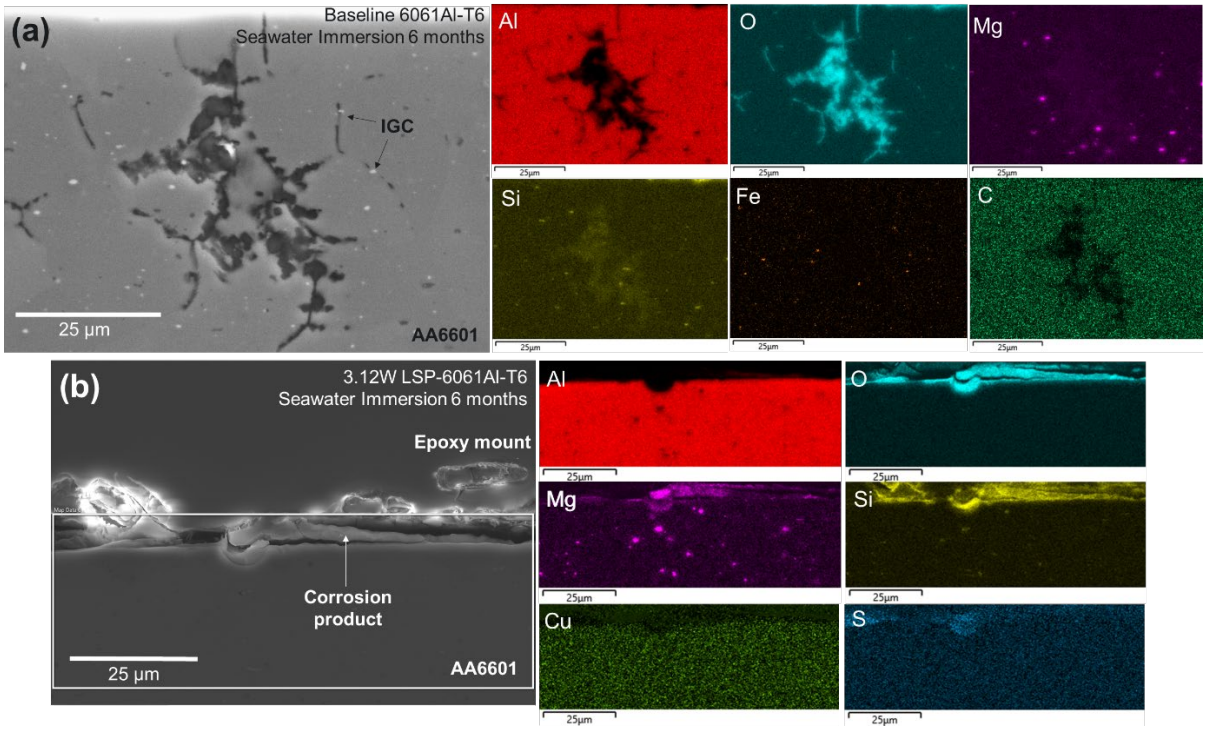

Figure 8: (a) Cross section of baseline non-LSP sample showing sub-surface intergranular corrosion (IGC) and its corresponding EDS maps, (b) Cross section of 3.12 W LSP sample showing absence of sub-surface intergranular corrosion and its corresponding EDS maps.

5.0 Summary & Conclusions

Current corrosion and antifouling surface protection methods involve the use of coatings that contain chemicals (organic biocides, Cu, etc.) that adversely affect marine life in several ways. LSP offers a more benign, non-chemical alternative to these existing surface protection methods by using a laser to modify the local surface chemistry and/or microstructure that enables the material to protect itself from corrosion and biofouling This further has the potential to reduce operational and maintenance costs and is not expected to adversely affect marine life. In this study, we explored 3 different LSP power inputs- 1.28 W, 2.34 W and 3.12 W to study the role of LSP on the susceptibility of AA6061 to corrosion and biofouling. This was done by immersing the samples in lab 3.5 wt.% NaCl solution and seawater for a period of 3 months and 6 months.

Under the testing conditions employed here, the main conclusions to date pertaining tests on 6061 Al are:

1. LSP samples did not show any evidence of sub-surface intergranular corrosion. In contrast, the baseline showed evidence of sub-surface intergranular corrosion and accompanying grain dissolution in its vicinity (Figure 8)

2. Laser surface processing is shown to reduce the magnitude of biofouling by as much as 40% (3.12 W LSP sample).

3. Exposure of the Al 6061 surface leads to an ~80x increase in weight of baseline coupons in natural seawater (corrosion + biofouling) as compared to the samples exposed to only corrosion in lab 3.5 wt.% NaCl solution (Figure 5). Biofouling species observed included algae, biofilm, barnacles, diatoms, and crustaceans, as shown in figures 6 and 7. The weight change (gain in the case for seawater exposed samples) can be understood by the combination of two factors- weight change induced due to corrosion in the seawater and weight change due to the adhered biofouling on the surface. This distinction was utilized to delineate the weight change due to corrosion and due to biofouling.

6.0 Proposed Future Steps

Corrosion in marine environments is a significant challenge and low-cost surface protection technologies are needed for greater penetration into marine energy sources. The following steps will be employed to further explore LSP for surface modification and to enable their implementation:

- Corrosion and biofouling studies on mild steel samples will be conducted using long term (up to 2 months) exposure to lab 3.5 wt.% NaCl solution and natural seawater, as reported for aluminum here.

- Resistance to abrasion of baseline and LSP samples will be investigated using wear / scratch resistance measurements performed in compliance with ASTM G133 at PNNL.

- Understanding the role of LSP on protection of treated surfaces when subject to galvanic coupling or in close proximity with electrochemically cathodic (in seawater) materials such as steel fasteners, nuts, etc.

- Analytical characterization will be performed to understand 1) how LSP modifies the native oxide layer, 2) LSP-induced introduction of new chemical species into the oxide (MgO/ZnO, etc.), and 3) dependence of sub-surface depth and recrystallization as a function of laser power. Such characterization can help us understand the fundamental mechanisms behind improved corrosion and biofouling resistance due to LSP.

7.0 References

[1] SketchandCalc, (n.d.). https://www.sketchandcalc.com/area-calculator-app/.

[2] C. Winner, Barnacles and Biofilms Could tiny predators help banish barnacles?, Oceanus. (2012). https://www.whoi.edu/oceanus/feature/barnacles-and-biofilms/.

[3] Marine Life Encyclopedia: Cephalopods, Crustaceans, & Other Shellfish- Acorn Barnacle, (n.d.). https://oceana.org/marine-life/acorn-barnacle/.

[4] S. Musabikha, I. Ketut Aria Pria Utama, Corrosion in the Marine Renewable Energy: A Review, Int. J. Environ. Res. Clean Energy. 7 (2017) 1–9. http://isomase.org/IJERCE1.php.

[5] H. Titah-Benbouzid, M. Benbouzid, Marine Renewable Energy Converters and Biofouling: A Review on Impacts and Prevention, A Rev. Impacts Prev. EWTEC. (2015) Paper 09P1-4-2. https://hal.archives-ouvertes.fr/hal-01199624.

[6] C.B. Panchal, Experimental Investigation of Marine Biofouling and Corrosion for Tropical Seawater, Fouling Sci. Technol. (1988) 241–247. https://doi.org/10.1007/978-94-009-2813-8_17.

[7] R. Miller, J. Loxton, Role of Biofouling in Marine Renewable Energy Development, in: 2016.

[8] B. Polagye, J. Thomson, Screening for Biofouling and Corrosion of Tidal Energy Device Materials: *In-situ* results for Admiralty Inlet, Puget Sound, Washington. Northwest National Marine Renewable Energy Center Techincal Memorandum. University of Washington, Seattle, WA, Un, Environ. Eng. (2010) 12.

[9] H. Qiu, K. Feng, A. Gapeeva, K. Meurisch, S. Kaps, X. Li, L. Yu, Y.K. Mishra, R. Adelung, M. Baum, Functional polymer materials for modern marine biofouling control, Prog. Polym. Sci. 127 (2022) 101516. https://doi.org/10.1016/j.progpolymsci.2022.101516.

[10] I. Omae, Organotin antifouling paints and their alternatives, Appl. Organomet. Chem. 17 (2003) 81–105. https://doi.org/10.1002/aoc.396.

[11] Washington State Department of Ecology, Antifouling Paints in Washington State Report and Recommendations Report to the Legislature, 2019.

[12] D. Claisse, C. Alzieu, Copper contamination as a result of antifouling paint regulations?, Mar. Pollut. Bull. 26 (1993) 395–397. https://doi.org/10.1016/0025-326X(93)90188-P.

[13] A.M. Prichard, Final decision concerning reevaluation of Copper based antifouling paint pesticides, 2018.

[14] M.Jamal. and X. Shi, Quality Assurance Project Plan: Performance Test of Green Alternatives to Copper Antifouling Paints, 2023.

Pacific Northwest National Laboratory

902 Battelle Boulevard
P.O. Box 999
Richland, WA 99354
1-888-375-PNNL (7665)

www.pnnl.gov